Entropy **2009**, *11*, 1025-1041; doi:10.3390/e11041025

OPEN ACCESS

entropy

ISSN 1099-4300

www.mdpi.com/journal/entropy

Article

On the Spectral Entropy of Thermodynamic Paths for Elementary Systems

Daniel J. Graham

Department of Chemistry, Loyola University Chicago, 6525 North Sheridan Road, Chicago, IL 60626, USA; E-Mail: dgraha1@luc.edu

Received: 13 October 2009 / Accepted: 27 November 2009 / Published: 7 December 2009

Abstract: Systems do not elect thermodynamic pathways on their own. They operate in tandem with their surroundings. Pathway selection and traversal require coordinated work and heat exchanges along with parallel tuning of the system variables. Previous research by the author (Reference [1]) focused on the information expressed in thermodynamic pathways. Examined here is how spectral entropy is a by-product of information that depends intricately on the pathway structure. The spectral entropy has proven to be a valuable tool in diverse fields. This paper illustrates the contact between spectral entropy and the properties which distinguish ideal from non-ideal gases. The role of spectral entropy in the first and second laws of thermodynamics and heat → work conversions is also discussed.

Keywords: entropy; information; thermodynamics; reversible transformations; fluid systems

PACS Codes: 05.10-a, 05.70.Ce, 64.10-+h, 82.60.-s

---

1. Introduction

By holding $K + 2$ variables constant, one controls the macroscopic state of a thermodynamic system. K equates with the number of components and at least one of the variables must be extensive. This axiom applies to solids, liquids, and gases at equilibrium [2]. In spite of the simplicity, a system's state point is not infinitely sharp. If it were, there would be no uncertainty in any quantities related to the control variables. Their measurements would afford zero thermodynamic information. This turns

out to be *almost* the case as discussed in several classics [3-5]. In Figure 1, the minor impact of fluctuations is summarized.

Panel A shows a closed, $K = 1$ gas in equilibrium with its surroundings. In the limit of ideal behavior, the density ρ is realized as:

$$\rho = \frac{\mathrm{N}}{\mathrm{V}} = \frac{p}{k_B T} \tag{1}$$

where N, V, p, and T are accessible macroscopic variables: particle number, volume, pressure, and temperature, respectively [6]. k_B is the Boltzmann entropy constant. Because of energy exchanges between the system and surroundings, ρ necessarily fluctuates about an average. It can be shown that the ratio between the density standard deviation σ_ρ and the average $<\rho>$ is [3-5]:

$$\frac{\sigma_\rho}{<\rho>} = \sqrt{\frac{k_B T \kappa_T}{V}} \tag{2}$$

κ_T is the isothermal compressibility:

$$\kappa_T = \frac{-1}{V}\left(\frac{\partial V}{\partial p}\right)_{T,N} \tag{3}$$

which reduces to $1/p$ for ideal behavior. In this simplest of examples, the Equation 2 ratio is especially compact, namely:

$$\frac{\sigma_\rho}{<\rho>} = \sqrt{\frac{k_B T \kappa_T}{V}} = N^{-1/2} \tag{4}$$

Substitutions based on typical gas conditions make the crucial point. If, say, $<\rho>$ were to equal 10^{23} particles/m^3 (*i.e.*, p ≈ 400 Pascals at room temperature), then $\sigma_\rho / <\rho> \approx 3 \times 10^{-12}$ and $\sigma_\rho \approx 3 \times 10^{11}$ particles/m^3. Three standard deviations of the number density (σ_ρ) would correspond to c. 10^{12} particles/m^3. Repeated laboratory measurements of ρ for a 1 m^3 volume would manifest a narrow distribution about the average. More than 99% of the readings would fall in the range 10^{23} +/− 10^{12} particles/m^3. A probability density plot based on the measurements would yield a near δ-function as in Panel B; higher density conditions only sharpen the function. If alternatively the ρ-time dependence were monitored, a recording as in Panel C would obtain. Here the particle density is shown to fluctuate about the average in a noisy fashion. A Fourier synthesis (or transform) would identify a zero-frequency (ω) component as the dominant one. The power spectrum in Panel D based on the Fourier analysis would evidence a single peak at ω = 0. Given the slight impact of energy exchanges between the system and surroundings, the amplitude is featureless and nearly zero for ω > 0.

Figure 1. Equilibrium Systems and Fluctuations. Panel A depicts a gas in equilibrium with its surroundings. Panel B shows the probability function that would obtain from repeated density measurements. Panel C illustrates the density behavior over time. Panel D shows the Fourier spectrum of the density behavior.

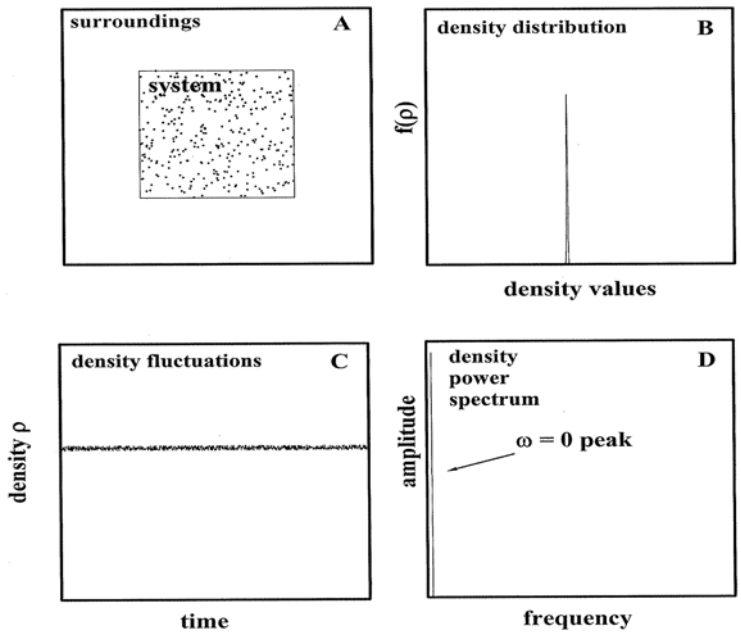

The Figure 1 message is that while the role of fluctuations is not visible in state equations such as Equation 1, it is a typically (*i.e.*, when ρ and V are appreciable) a very minor one. Thus ρ quantified via Equation 1 and similar can be viewed as the overwhelmingly most probable value. Parallel arguments can be constructed for other state quantities such as the pressure p, chemical potential μ, and entropy S. The sources of non-ideality, namely interactions between the particles, do not alter the message. The exception would be when the state point falls in the neighborhood of a phase boundary.

An individual state point poses little uncertainty regarding thermodynamic quantities. Multiple connected points paint an altogether different picture. This is the subject of Figure 2. If control variables such as p and V are tuned, a system is directed along a pathway that threads nearest neighbor state points. The pathway can be elementary as in isothermal, adiabatic, and isochoric transformations where T, S, and V, respectively, are constant. Yet the path need not be a proper function at all as in Panel B. Tuning p and V accesses an infinitude of states that link the initial to the final. Whether simple or complicated, a pathway allows for alternative representations using variables such as T, ρ (Panels C and D) and more. Thermodynamic pathways form a time-honored subject [7]. They continue to warrant study as model algorithms and computational programs. At a root level, thermodynamic pathways characterize step-wise parallel programming on the part of a system and its surroundings. The algorithms are executed via simultaneous tuning of variables tied to the work and heat exchanges.

Figure 2. Systems and Variable Tuning. Panel A shows a system in which pressure and volume are tuned in parallel with work and heat exchanges. Panel B illustrates one of infinite possible pathways that connect the initial and final states. Panels C and D present alternative representations of the pathway. For simplicity, the system has been taken to be 1.00 mole of a monatomic ideal gas. The use of liter and atmosphere units follows the practice of classic thermodynamic texts [2,6,7].

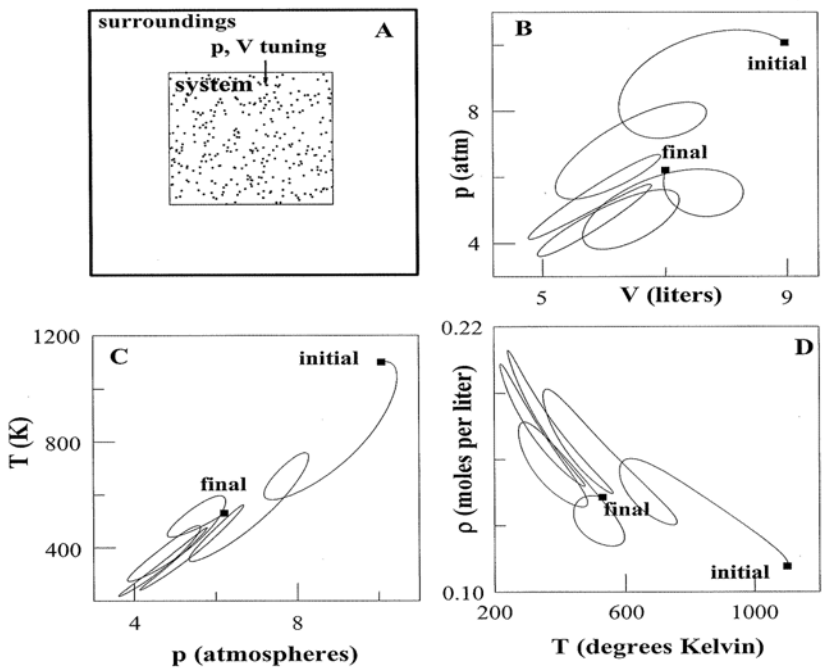

Information is the lifeblood of programs and algorithms. It is an imbedded feature of all thermodynamic pathways. The scenarios are much in contrast with individual state points such as in Figure 1 where a measurement traps very little information. Information in connection with thermodynamic pathways was explored by the author in a previous work [1]. It was shown how a locus of nearest neighbor state points predicates a type of probability space. Objective queries of the system offer information in amounts significantly greater than for any single point. The amounts depend intricately on the pathway structure, measurement resolution, and system composition.

This paper takes another step by examining the spectral entropy allied with a pathway. This quantity also proves connected with collections of nearest neighbor states. Importantly, the spectral entropy identifies novel distinctions between ideal and non-ideal gases. It connects as well with the constraints placed by the first and second laws of thermodynamics. A pathway's spectral entropy highlights the optimum programming strategies for heat → work conversions. One notes the spectral entropy to provide a powerful tool in diverse fields. To cite only a few, it has found judicious applications in speech recognition algorithms, genome analysis, and particle motion research [8-10]. To the author's knowledge, the present study examines a first link between the spectral entropy and thermodynamic pathways. While thermodynamics enjoys a highly-developed infrastructure, new theoretical and experimental tools continue to be discovered [11]. Moreover, topics that are closely

related to spectral entropy include heat engines, system fluctuations, and non-ideal gases. These have been well represented the past few years in this journal [12–16].

2. Thermodynamic Pathways, Information, and Spectral Entropy

Figure 3 illustrates how information is expressed by a pathway. For simplicity, the system is taken to be a closed one composed of 1.00 mole of a monatomic ideal gas. Let the system be transformed along a path in the pV plane that matches the one illustrated in Figure 2. Transformations do not occur by themselves. Thus the upper portion of Figure 3 schematically depicts the requisite parallel and serial programming by way of an entry $\{p_i, V_i\}$ sequence. In effect, ordered pairs of p_i, V_i enable the system to be stepped precisely along a chosen pathway. There is more than one input program which can accomplish the task. The $K + 2$ criterion for specifying state points allows other control variable pairs and sequences to be equally effective: $\{p_i, T_i\}$, $\{\rho_i, V_i\}$, and so forth.

The pathway in Figure 3 is clearly reversible. This means that the closed system maintains equilibrium with the surroundings at all stages. A non-equilibrium condition would indeed not correspond to any single point in the pV, $T\rho$, or other variable plane. Pathways articulate the initial, final, and intermediate states. Then if the equation of state is known, the differences between the numerous functions of state can be quantified: entropy S, free energy G, internal energy U, and more. Quantities that instead hinge on the pathway structure details can also obtain: work received W_{rec} and heat received Q_{rec}.

Reversible pathways yield many thermodynamic quantities. They are devoid of temporal data, however, on account of their equilibrium nature. All of the states are spelled out via an input program, but they lack qualifiers on their time and duration of access. Therefore if an objective experimenter who is knowledgeable of the state point locus, but ignorant of temporal details, inquires "Does the system pressure p at present fall in the following range?":

$$p_i \leq p \leq p_i + \Delta p \tag{5}$$

the answer would be uncertain in advance of measurement via a suitable transducer (represented by a triangle in Figure 3) such as a McLeod gauge. In taking the pathway states to be equally probable, the likelihood of an affirmative answer—the conversion of uncertainty "?" to "yes" in Figure 3, depends on the number of states that meet the above criterion. Note how for the pathway appearing in the lower half of Figure 3, the likelihood of p meeting the condition in (5) is greater than for:

$$p_j \leq p \leq p_j + \Delta p \tag{6}$$

As indicated by the enhanced blackening of pathway segments, there are about eight times the quantity of state points that meet the condition in (5) as compared with (6).

Figure 3. Pathways and Information. The upper portion schematically illustrates how a control variable sequence $\{p_i, V_i\}$ operates as a thermodynamic algorithm for pathway traversal: ordered pairs p_i, V_i enable the system to be stepped precisely through a succession of state points. Measurements via a transducer (triangle symbol) such as a McLeod gauge reduce uncertainty ? and trap information about the system, *i.e.*, convert "?" to "yes" or "no". The amount of information depends on the number and distribution of pathway state points.

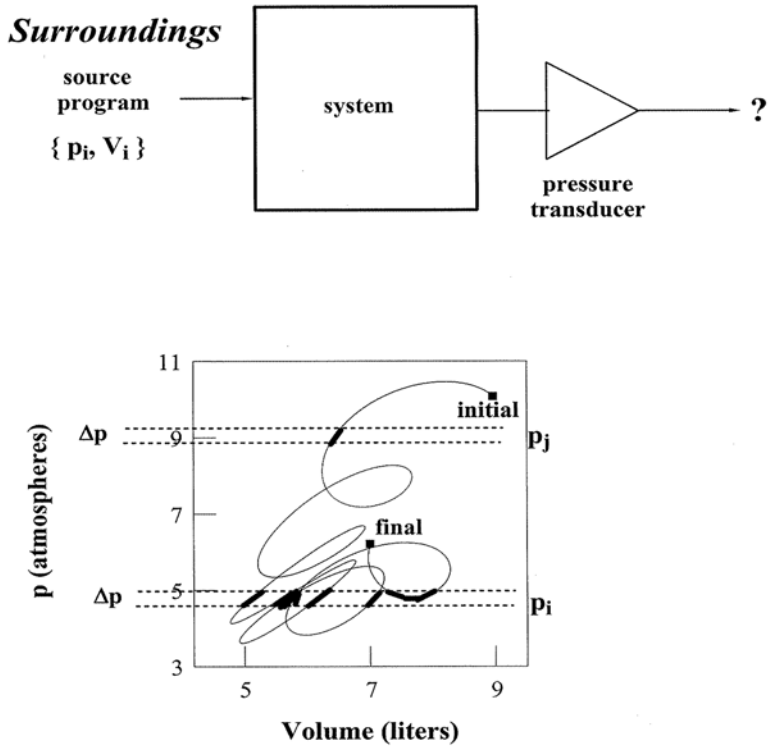

It was shown in previous research how to quantify the likelihood of "yes" *versus* "no" answers to state queries [1]. The procedure involved computing the pathway length over the states that meet the query conditions via line integrals. The pieces are summed and weighed against the total pathway length. The results include sets of probability values and surprisals: $\{ prob_i \}$ and $\{-\log_2 prob_i \}$, respectively. The expectation value of the surprisals quantifies the pathway information I_Y in bits:

$$I_Y = -\sum prob_i \log_2 prob_i \tag{7}$$

where the subscript Y denotes the thermodynamic quantity queried such as $Y \leftrightarrow p$ in Figure 3. I_Y is enhanced if the number of terms in Equation 7 is increased. This would be brought about by augmenting the pathway, or by extending the measurements at higher resolution—narrower Δp. I_Y would be further enhanced if the probability terms proved equal (or nearly so) in value; this applies typically to pathways that evince complex structures. I_Y is zero for certain quantities for certain pathways: isobaric, isothermal, and adiabatic pathways are absent in $Y \leftrightarrow p$, T, and S information, respectively. All closed systems pose zero information regarding the particle number: $I_{Y \leftrightarrow N} = 0$.

The spectral entropy S_Y is an immediate by-product of information. There indeed exists S_Y computable for every pathway state property, *i.e.*, $Y \leftrightarrow p$, V, T, U, G, S, *etc*. Unlike information,

S_Y does not stem from yes/no queries and measurements with thermometers, pressure gauges, and so forth. Its significance arises instead because of the contact made with the algorithmic structure. Most notably, S_Y quantifies the symmetry, or lack of it, imbedded in a pathway. Figure 4, for example, shows how S_Y originates for $Y \leftrightarrow p$, the pressure tuning of a system with commentary as follows.

Whether simple or complex, a thermodynamic pathway always admits a parametric representation. In such a way, dimensionless λ operates as an independent variable common to all state quantities. Panels A and B in Figure 4 show the pressure behavior over the same path charted in Figure 3. There is a one-to-one correspondence of λ to each state point as indicated by the dotted lines. This correspondence holds for V and all other quantities T, S, *etc*., traversed by the path.

As is universally appreciated, algorithms and programs can be executed multiple times. Thus to quantify S_Y, a thermodynamic pathway is regarded as expressing a state space period of $2L$. The periodicity allows each λ-dependent function to be written as a Fourier series [17]. For instance, the pressure function of Figure 4 can be re-expressed as:

$$p(\lambda) = a_o + \sum_n \{a_n \cos\left(\frac{n\pi\lambda}{L}\right) + b_n \sin\left(\frac{n\pi\lambda}{L}\right)\} \tag{8}$$

where:

$$a_o = \frac{1}{2L}\sum_{\lambda=-L}^{\lambda=+L} p(\lambda)\Delta\lambda \tag{9A}$$

$$a_n = \frac{1}{L}\sum_{\lambda=-L}^{\lambda=+L} p(\lambda)\cos\left(\frac{n\pi\lambda}{L}\right)\Delta\lambda \tag{9B}$$

$$b_n = \frac{1}{L}\sum_{\lambda=-L}^{\lambda=+L} p(\lambda)\sin\left(\frac{n\pi\lambda}{L}\right)\Delta\lambda \tag{9C}$$

The arguments of the trigonometric functions define "frequencies":

$$\chi_n = \frac{n\pi}{L} \tag{10}$$

The quotation marks emphasize that the χ_n have nothing to do with time as with ω in Figure 1. The χ_n rather identify the density of the pathway kinks governed by the program. The pathway of Panel A demonstrates twists and turns in both pressure and volume. Their Fourier representations accordingly necessitate multiple terms with diverse χ_n. By contrast, an isobaric or isochoric pathway demonstrates constant p or V, respectively. In such cases, $p(\lambda)$ or $V(\lambda)$ require only a single term in their Fourier expressions at $\chi_o = 0$. Each representation is equivalent to that for a single state point.

Figure 4. Pathways and Spectral Entropy. Panels A and B show how a pathway admits a parametric representation. The representation can be expressed as a Fourier sum of trigonometric functions such as shown as in Panel C. The weight coefficients compose a power spectrum as in Panel D.

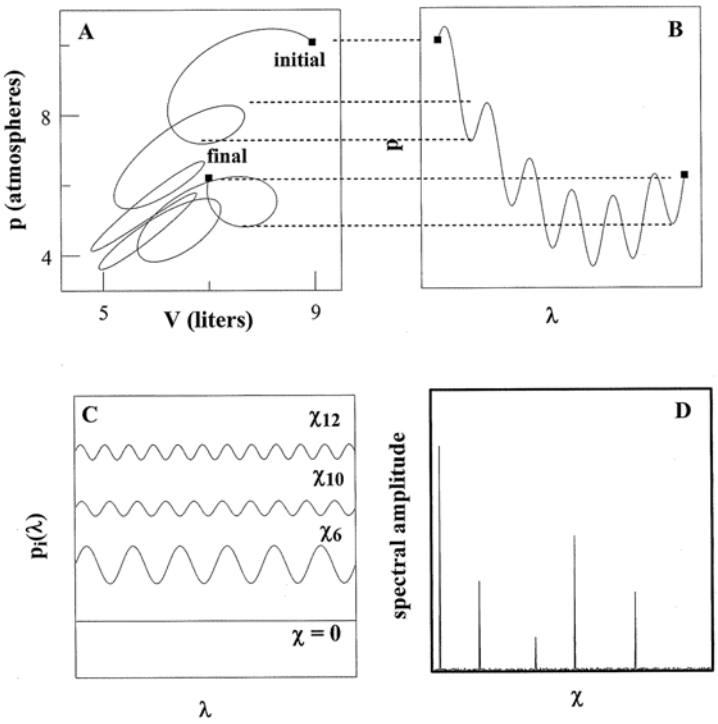

The coefficients a_n, b_n determine the degree to which each Fourier term contributes. The modulus quantity:

$$A_n = \sqrt{a_n^2 + b_n^2} \tag{11}$$

then identifies the amplitude allied with each χ_n. A plot of A_n *versus* χ_n realizes a power spectrum as in Panel D. At infinite resolution (infinitesimal Δp), Equations 8 and 9 converge to integrals which predicate an infinite number of spectral terms. A finite-step pathway is, of course, much closer to experimental reality.

Figure 5 illustrates an example of the spectral entropy $S_{Y\leftrightarrow p}$ that results from pressure tuning of a system: The calculation follows from the pathway of Figure 4 that is, in turn, described by the (arbitrarily chosen) parametric function:

$$p(\lambda) = B \cdot \left[10 + \lambda^{2.2} - 5\lambda + \sin\left(\frac{12\pi\lambda}{3} \right) \right] \tag{12}$$

λ is dimensionless while B equates with the unit pressure, here assigned to be 1.00 atmosphere. The Fourier representation has been computed using Equations 8 and 9 and its normalized power spectrum

is contained in the lower panel of Figure 5. In calculating the spectrum, the A_n have been rescaled by factor ξ so that:

$$\xi \sum_n A_n = 1 \tag{13}$$

Clearly the spectrum reflects a non-trivial component distribution that is heavily weighted at low χ_n. $S_{Y\leftrightarrow p}$ follows straightaway, viz.

$$S_{Y\leftrightarrow p} = -\sum_n \xi A_n \log_2(\xi A_n) \tag{14}$$

The summation is dictated by the number of Fourier components: 100 are more than sufficient given the typical pathway bias toward low χ_n and finite resolution. The logarithmic terms of Equation 14 are analogous to information surprisal quantities [18]. Each term is weighted by a normalized amplitude which is analogous to a probability term. The results of the weighted summation appear in the upper panel of Figure 5. The results for $S_{Y\leftrightarrow V}$ have been included for comparison. One observes that different thermodynamic quantities of the identical pathway need not express the same spectral entropy. The "bit" units are applicable in the same way as information. For this single, arbitrarily-chosen pathway—there are infinite possible—it requires approximately 5 bits to encode the amplitude terms in the *p*, *V* power spectra.

Figure 5. Power Spectra and Weighted Surprisal Sums. The lower panel illustrates the normalized power spectrum based on p(λ) of Figure 4. The upper panel illustrates the weighted sum of surprisals for pressure and volume pathway variables.

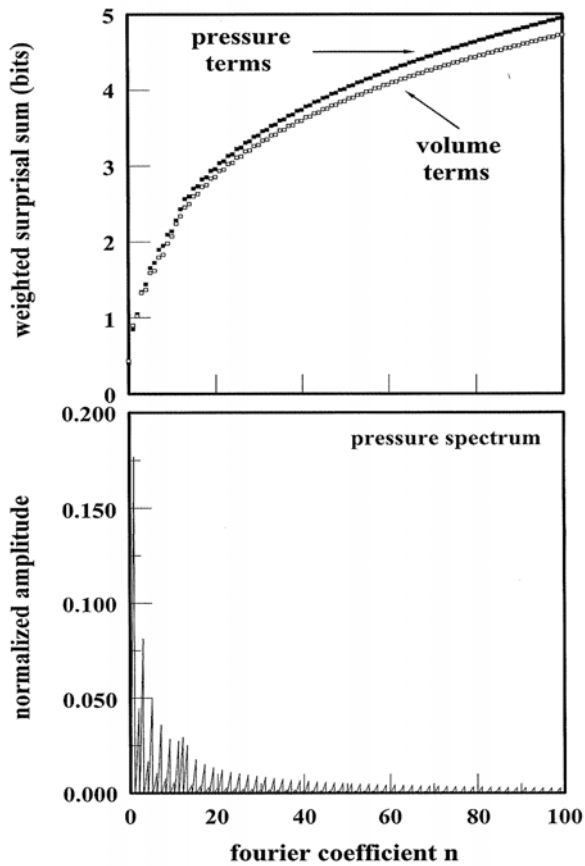

3. Applications and Discussion

The spectral entropy has been employed in diverse research [8-10]. Concerning thermodynamic pathways, S_Y contributes insights in four respects. The first concerns the properties that distinguish ideal from non-ideal gases. As is well known, the former demonstrates signature features beginning with Equation 1. Additional ones include that the internal energy U and enthalpy H depend solely on N and T [6,7]. For a monatomic ideal gas:

$$U = \frac{3Nk_BT}{2} \tag{15}$$

and:

$$H = U + pV \tag{16}$$

$$= \frac{5Nk_BT}{2}$$

It follows that for ideal systems, the heat capacities C_V, C_p are independent of volume and temperature:

$$C_V = \left(\frac{\partial U}{\partial T}\right)_{V,N} \tag{17}$$

$$= \frac{3Nk_B}{2}$$

and:

$$C_p = \left(\frac{\partial H}{\partial T}\right)_{p,N} \tag{18}$$

$$= \frac{5Nk_B}{2}$$

Other response functions such as the coefficient of thermal expansion α_p and isothermal compressibility κ_T (Equation 3) are equally simple:

$$\alpha_p = \frac{1}{V}\left(\frac{\partial V}{\partial T}\right)_{p,N} \tag{19}$$

$$= \frac{1}{T}$$

and $\kappa_T = 1/p$. A non-ideal system requires more complicated mathematics for the state relations. The van der Waals equation is a well-established, elementary model for interacting gases [6,7,16]:

$$p = \frac{Nk_BT}{V - Nb} - \frac{aN^2}{V^2} \tag{20}$$

where a and b scale, respectively, with the attractive and repulsive forces between the particles. Note that conventional notation is being used in Equation 20 and beyond. The van der Waals a and b

coefficients are not to be confused with the Fourier weight coefficients of Equations 9 and 11. Then with Equation 20, or similar non-ideal equation of state operative, the representations of potentials U and H are no longer so compact. In the van der Waals case:

$$U = \frac{3Nk_BT}{2} - \frac{aN^2}{V} \tag{21}$$

while:

$$H = \frac{3Nk_BT}{2} - \frac{2aN^2}{V} + \frac{Nk_BTV}{V - Nb} \tag{22}$$

C_V for a van der Waals system is equivalent to that appearing in Equation 17. C_p does not demonstrate the same economy, however:

$$C_p = C_V + \frac{\alpha_p^2 VT}{\kappa_T} \tag{23}$$

where:

$$\alpha_p = \frac{Nk_BV}{3pV^2 - 2pNbV + aN^2 - 2Nk_BVT} \tag{24}$$

$$\kappa_T = \frac{V^2 - NbV}{3pV^2 - 2pNbV + aN^2 - 2Nk_BVT} \tag{25}$$

The take-home points are as follows. There are established properties that distinguish ideal from non-ideal gases. To the list need to be added three additional:

(1) Ideal and non-ideal samples alike express $S_{Y\leftrightarrow T} = 0$ for isothermal pathways. Yet only an ideal gas expresses zero $S_{Y\leftrightarrow U}$ and $S_{Y\leftrightarrow H}$ for isothermal pathways.

(2) *All* pathways—no exceptions—for a closed ideal system express zero $S_{Y\leftrightarrow CV}$ and $S_{Y\leftrightarrow Cp}$. In sharp contrast, only highly select ones demonstrate zero $S_{Y\leftrightarrow Cp}$ for non-ideal systems. This is because C_p depends non-trivially on p, T, V, a, and b as in Equations 23, 24, and 25.

(3) If a system is ideal, its isothermal and isobaric pathways pose zero $S_{Y\leftrightarrow \alpha p}$ and $S_{Y\leftrightarrow \kappa T}$, respectively. Matters are more complicated for a non-ideal system. Zero $S_{Y\leftrightarrow \alpha p}$ and $S_{Y\leftrightarrow \kappa T}$ can only be demonstrated by highly rarefied pathways. This is because κ_p and α_T depend intricately on p, T, and V, and case-specific a and b. The zero $S_{Y\leftrightarrow \alpha p}$ and $S_{Y\leftrightarrow \kappa T}$ pathways programmed for an argon sample would not apply to neon.

The above can be demonstrated via numerous equations of state, not simply the van der Waals, that address the effects of interparticle forces. Even so, real materials conduct themselves ideally at sufficiently low densities and high temperatures. Hence the features 1–3 are universal in their application. The second and third are especially striking. To construct a pathway with fixed heat capacity is trivial for an ideal gas–any and all pathways will do. To engineer likewise for a non-ideal material, however, incurs infinitely greater programming costs. Regarding (3), to ascertain a system's

thermodynamic properties, knowledge of *either* C_V or C_p along a pathway that threads a range of p and T is required [6]. Usually C_p is experimentally more accessible via the specific heat c_p:

$$C_p = mc_p \tag{26}$$

where m is the system mass. Equation 26 plus Feature (2) inform the experimenter, however, that the accessibility of C_p obtains at the price of greater pathway complexity for a non-ideal system. One way of quantifying the complexity is via $S_{Y\leftrightarrow Cp}$.

Along related lines, knowledge of *both* α_p and κ_T is required at *all* points in a region of state space in order to realize the thermodynamic quantities U, G, S, *etc*. [6]. From Feature (3), one learns that it is impossible to measure α_p or κ_T for *one* state of a non-ideal system and thereby automatically know the values for points along the intersecting isotherms and isobars in the state space. As with C_p, the complexity of α_p and κ_T is non-trivial for real systems, yet it is directly quantified by $S_{Y\leftrightarrow\alpha p}$ and $S_{Y\leftrightarrow\kappa T}$.

The second insight relates pathway spectral entropy to the first law of thermodynamics. This law holds that the internal energy change ΔU of any system equates with the work and heat received:

$$\Delta U = W_{rec} + Q_{rec} \tag{27}$$

with special cases applying to isochoric (W_{rec} = 0) and adiabatic (Q_{rec} = 0) transformations [1,5,6]. The first law contact with pathway spectral entropy is notably different. Specifically $S_{Y\leftrightarrow Wrec}$ and $S_{Y\leftrightarrow Qrec}$ *bracket* $S_{Y\leftrightarrow\Delta U}$:

$$S_{Y\leftrightarrow Wrec} \leq S_{Y\leftrightarrow\Delta U} \leq S_{Y\leftrightarrow Qrec} \tag{28}$$

and:

$$S_{Y\leftrightarrow Qrec} \leq S_{Y\leftrightarrow\Delta U} \leq S_{Y\leftrightarrow Wrec} \tag{29}$$

In so doing, the spectral entropy of the work and heat exchanges provides upper and lower bounds for $S_{Y\leftrightarrow\Delta U}$. There is a single exception, namely when W_{rec} and Q_{rec} exactly cancel at all points of a pathway; this renders $S_{Y\leftrightarrow\Delta U}$ zero. More importantly, for isochoric and adiabatic pathways, (28) and (29) become equality statements:

$$S_{Y\leftrightarrow Qrec} = 0\,;\, S_{Y\leftrightarrow\Delta U} = S_{Y\leftrightarrow Wrec} \tag{30}$$

$$S_{Y\leftrightarrow Wrec} = 0\,;\, S_{Y\leftrightarrow\Delta U} = S_{Y\leftrightarrow Qrec} \tag{31}$$

The first law bearing on pathway spectral entropy is crucial. It emphasizes how the work and heat exchanges between a system and surroundings must be programmed in-parallel with each other. $S_{Y\leftrightarrow\Delta U}$ could exceed *both* $S_{Y\leftrightarrow Wrec}$ and $S_{Y\leftrightarrow Qrec}$ only if the exchanges were independent, thus admitting different sets of Fourier coefficients. The first law and the nature of reversible pathways preclude this. For one of infinite possible examples, Figure 6 illustrates the weighted surprisal summations that yield $S_{Y\leftrightarrow Wrec}$, $S_{Y\leftrightarrow\Delta U}$, and $S_{Y\leftrightarrow Qrec}$ for the Figure 4 pathway. In this case, the condition in (28) holds. Evidently the complexity of programmed heat exchanges exceeds that of the work exchanges. Such a trait is not apparent from casual inspection of the pathway structure.

Figure 6. Weighted Surprisal Sums based on ΔU, W_{rec}, and Q_{rec} Power Spectra. The data derive from the pathway illustrated in Figure 4.

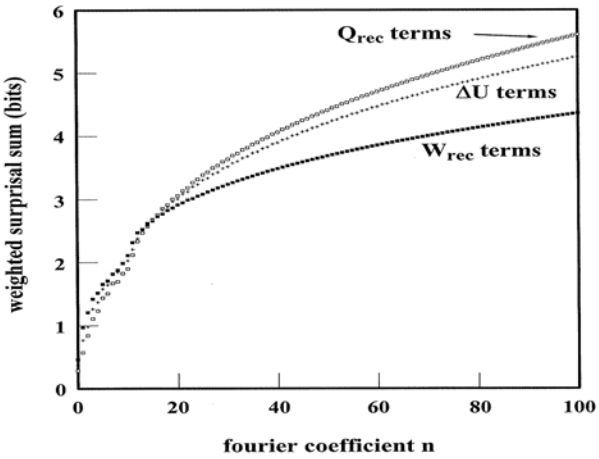

The second law of thermodynamics also impacts the spectral entropy; this is the subject of Figure 7. The Caratheodory statement of the second law asserts that there exist neighboring states of a system which are impossible to access along an adiabatic path [19]. A pathway's spectral entropy admits a parallel statement:

All systems possess neighboring states for which a $S_{Y\leftrightarrow S} = 0$ path is non-existent. Figure 7 shows four (of *infinite* possible) arrows that pinpoint nearby states. For these, there exists no $S_{Y\leftrightarrow S} = 0$ pathway that links the initial state without expression of positive $S_{Y\leftrightarrow S}$. The Caratheodory principle emphasizes that adiabatic pathways are exceptional for systems, ideal and otherwise. The same principle establishes the rarity of $S_{Y\leftrightarrow S} = 0$ pathways.

Figure 7. Pathways and Neighboring States. The arrows point to several (of infinite possible) neighboring states that *cannot* be accessed by an adiabatic/isentropic path. The pathway identifies one (of infinite possible) that can link initial and final states. It is virtually always the case that changing paths incurs changes in the spectral entropy.

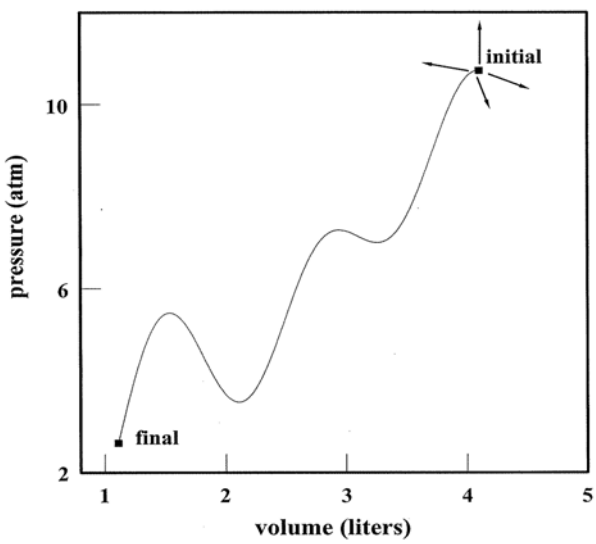

There follows a corollary:
There exist an infinite number of pathways that are able to link an initial to a final state. The curve in Figure 7 represents one (of infinite possible) having positive $S_{Y\leftrightarrow S}$, $S_{Y\leftrightarrow V}$, $S_{Y\leftrightarrow p}$, *etc*. There exist *neighboring pathways* for which a *non-zero change* in S_Y is impossible: $Y \leftrightarrow p$, T, U, μ, *etc*. The reason is that altering a pathway inexorably modifies one or more weight coefficients in the Fourier representation. Neighboring states that admit fixed-entropy pathways are special by the Caratheodory principle. Neighboring pathways that pose zero change in the spectral entropy prove no less special.

Figure 8. Carnot Cycles and Pathways. A Carnot cycle for 1.00 mole of monatomic ideal gas is illustrated in both the *pV* and *TS* planes. The Carnot strategy in relation to pathway spectral entropy is discussed in the text.

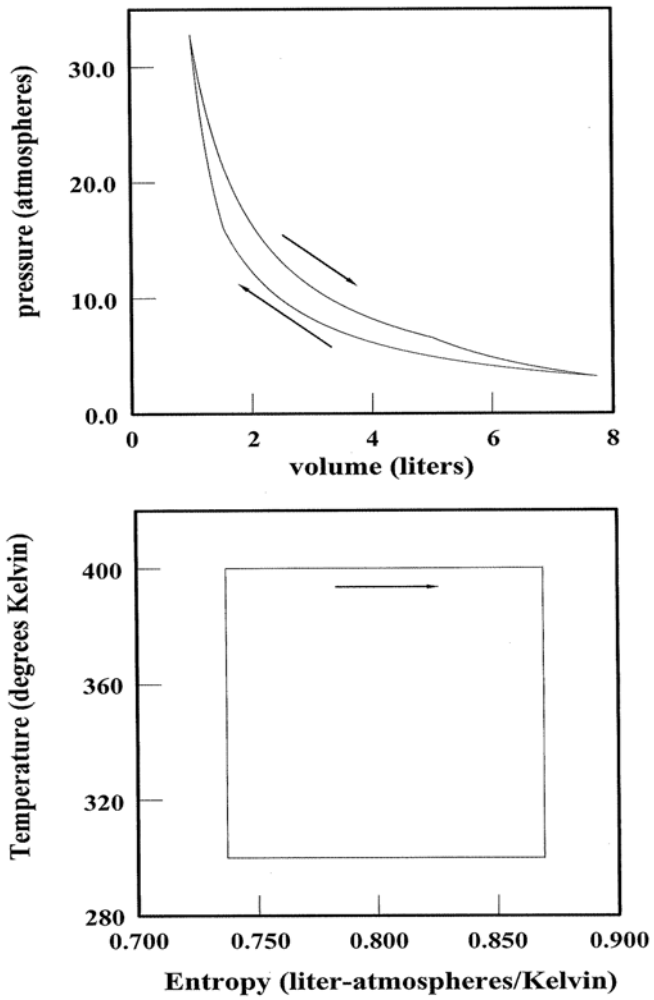

A final insight concerns heat engines, devices that transform a system along a cyclic pathway such that the initial and final states are identical. In simplest terms, heat is injected into the system (e.g., steam or combustion gas mixtures) at some high temperature; entropy is injected simultaneously. So that mechanical integrity is preserved, an equivalent amount of entropy must be ejected by the system somewhere along the pathway. The only feasible way is for the system to cast out "wasted" heat at some lower temperature. It follows that the conversion efficiency of injected heat → output work can never be 100%. The output work is at best equal to $Q_{injected}$–Q_{wasted} [6,7].

Not all cyclic transformations are created equal. Thus Carnot identified the optimum pathways for heat → work conversions [6,7,12,13]. These entail minimizing the thermal gradients within the system while maximizing the temperature differences between the points of heat injection and ejection. The first strategy minimizes the irreversibilities that create *additional* entropy; this extra entropy must also be ejected at some point of the cycle to maintain integrity. The latter strategy enhances the ejection efficiency as ΔS scales inversely with temperature. One example of a Carnot cycle is represented in Figure 8. Shown for both the pV and TS planes are the state point loci for 1.00 mole of a monatomic ideal gas operating over a temperature range of 300–400 K. Heat is injected along the upper isotherm while ejection occupies the lower. The work performed over each cycle equates with the area enclosed by each cyclic pathway.

Figure 9. Cyclic Pathways and Spectral Entropy. Upper and lower panels illustrate highly similar cyclic pathways for 1.00 mole of monatomic ideal gas. The *volume* domains are identical while the pressure domains are nearly so. The heat → work conversion efficiency is greater—25% *versus* 12%—for the cycle in the lower panel because $S_{Y\leftrightarrow TS}$ for the **B** segment is less than that for **A**.

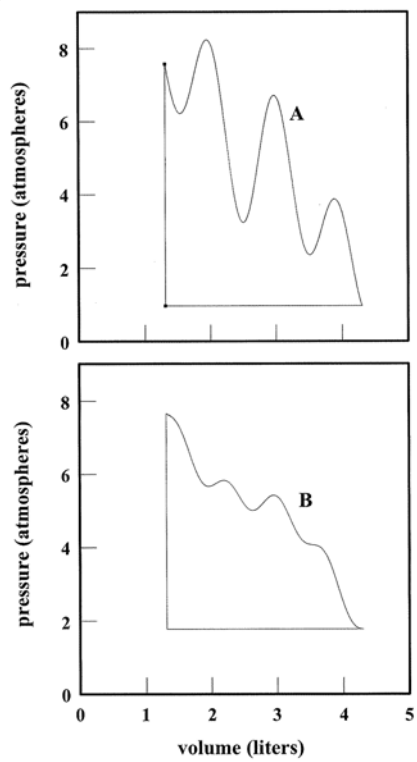

Carnot's strategy can be stated succinctly in spectral entropy terms:
At all points of the cyclic pathway, the following equality must be maintained:

$$S_{Y\leftrightarrow T} + S_{Y\leftrightarrow S} = S_{Y\leftrightarrow TS} \tag{32}$$

$S_{Y\leftrightarrow T}$ and $S_{Y\leftrightarrow S}$ are respectively zero for isothermal and adiabatic pathways. Thus Equation 32 reflects that the optimum algorithm for heat → work conversions is where $S_{Y\leftrightarrow TS}$ is limited *either* by $S_{Y\leftrightarrow T}$ or $S_{Y\leftrightarrow S}$. In effect, $S_{Y\leftrightarrow T}$ and $S_{Y\leftrightarrow S}$ establish an upper bound for $S_{Y\leftrightarrow TS}$ so as to minimize the spectral entropy. In other words, the pathway $S_{Y\leftrightarrow TS}$ must demonstrate a single source of thermal

programming complexity for the maximum efficiency. Clearly all the pathway segments of Figure 8 demonstrate this critical property. The condition is unmodified if the segments are subdivided arbitrarily. Note the Carnot segments to be radically different from the pathways illustrated of the previous figures where:

$$S_{Y\leftrightarrow T} + S_{Y\leftrightarrow S} > S_{Y\leftrightarrow TS} \tag{33}$$

The *TS*-spectral entropy provides an alternative assessment of pathway segments for their suitability in heat engine programs. As an example, Figure 9 shows two (of infinite possible) cyclic pathways that have equivalent volume domains and nearly-equal pressure domains. The upper segments A and B are different, however. The heat → work conversion efficiencies are readily computed by conventional methods. Alternatively, a calculation of $S_{Y\leftrightarrow TS}$ for the A and B segments immediately identifies the more efficient program. $S_{Y\leftrightarrow TS}$ is ca. 10% less for B in the lower panel; the heat → work conversion efficiency is about double that for the upper panel cycle. This holds in spite of the nearly-double temperature domain covered in the upper cycle.

4. Summary and Closing Comments

Systems do not elect and travel pathways by themselves. Joint operations with the surroundings are required. These entail highly-coordinated work and heat exchanges and parallel tuning of the system variables. Algorithms and programs form the currency for these operations. The spectral entropy for several variables was examined for elementary systems and algorithms. Shown was how S_Y distinguishes ideal from non-ideal gases; it connects as well with the first and second laws and the optimal programs encoded for heat engines. This paper focused on the pathway spectral entropy for elementary macroscopic systems. Clearly algorithms and programs are distinguished by their entropic character. Therefore a follow-up task is to identify the *minimum* S_Y—pathways that direct a thermodynamic state toward another. Such research is currently in progress. It is further noteworthy that microscopic systems such as enzymes present thermodynamic fluctuations and pathways under dynamic, non-equilibrium conditions [20,21]. The pathways of these systems might benefit from an analysis in spectral entropy terms. The properties described here for non-ideal systems, and first and second law constraints offer valid starting points.

Acknowledgements

The author is grateful to Miriam Kim and Matthew Sara for survey calculations during the initial stages of the project. Also appreciated is support of this work from the Department of Chemistry, Loyola University Chicago. The author thanks anonymous reviewers for helpful comments and criticism.

References and Notes

1. Graham, D.J.; Kim, M. Information and classical thermodynamic transformations. *J. Phys. Chem. B* **2008**, *112*, 10585-10593.

2. Denbigh, K. *The Principles of Chemical Equilibrium*, 3rd ed.; Cambridge University Press: London, UK, 1971; Chapter I.
3. Landau, L.D.; Lifshitz, E.M. *Statistical Physics*, 2nd ed.; Addison-Wesley: Reading, PA, USA, 1969; Chapter XII.
4. Kauzmann, W. *Thermodynamics and Statistics*; W.A. Benjamin, Inc.: New York, NY, USA, 1967; Chapter 4.
5. Kittel, C. *Elementary Statistical Physics*; Dover Publications: New York, NY, USA, 2004; Part II.
6. Desloge, E.A. *Thermal Physics;* Holt, Rinehart and Winston: New York, NY, USA, 1968; Chapters 13, 19, and 20 were most helpful to this research.
7. Fermi, E. *Thermodynamics*; Dover Publications: New York, NY, USA, 1956; Chapter 1.
8. Lee, W.-S.; Roh, Y.-W.; Kim, D.-J.; Kim, J.-H.; Hong, K.-S. Speech emotion recognition using spectral entropy. *Lect. Notes Comput. Sci.* **2008**, *5315*, 45-54.
9. Chechetkin, V.R.; Lobzin, V.V. Spectral entropy criteria for structural segmentation in genomic DNA sequences. *Phys. Lett. A* **2004**, *328*, 79-86.
10. Powell, G.E.; Percival, I.C. A spectral entropy method for distinguishing regular and irregular motion of Hamiltonian systems. *J. Phys. A* **1979**, *12*, 2053-2071.
11. Zhou, S. Reformulation of liquid perturbation theory for low temperatures. *Phys. Rev*. **2009**, *E79*, 011126.
12. Muller, A.W.J. Emergence of animals from Heat Engines-Part 1. Before the snowball earths. *Entropy* **2009**, *11*, 463-512.
13. Feidt, M. Optimal thermodynamics—New upperbounds. *Entropy* **2009**, *11*, 529-547.
14. Chang, Y.-F. Entropy, fluctuation magnified and internal interactions. *Entropy* **2005**, *7*, 190-198.
15. Gordon, L.G. The Decrease in Entropy via Fluctuations. *Entropy* **2004**, *6*, 38-49.
16. Ladino-Luna, D. Van der Waals gas as working substance in a Curzon and Ahlborn-Novikov engine. *Entropy* **2005**, *7*, 108-121.
17. Churchill, R.V. *Fourier Series and Boundary Value Problems*; McGraw-Hill: New York, NY, USA, 1941; Chapters IV and V.
18. Kullback, S. *Information Theory and Statistics*; Dover Publications: New York, NY, USA, 1968; Chapter I.
19. Chandrasekhar, S. *An Introduction to Stellar Structure*; Dover Publications: New York, NY, USA, 1967; Chapter I.
20. Cooper, A. Thermodynamic fluctuations in protein molecules. *Proc. Natl. Acad. Sci. USA* **1976**, *73*, 2740-2741.
21. Warshel, A. *Computer Modeling of Chemical Reactions in Enzymes and Solutions*; Wiley: New York, NY, USA, 1991.